INVESTIGATE AND COMPARE ANALYSIS METHOD OF HAMMERHEAD BRIDGE PIER CAPS

*Wana Dagim, ** S.Karunanidhi,
*Civil Engineering Department, College of Engineering, Assosa University, Ethiopia
Email: dursa2712@gmail.com
**Civil Engineering Department, College of Eng`g &Tech, Wollega University, Ethiopia
Email: karunabalasingam@gmail.com

ABSTRACT: *In reinforced concrete structures the engineer often faced with regions of a structure that contains discontinuities, such as abrupt changes in geometry or the presence of concentrated loads and reactions. The presence of a discontinuity results in a disturbance in the flow of stresses in regions adjacent to the discontinuity and therefore these regions are referred to as "disturbed regions". One factor that contributes to the structural deficiency of a bridge is lack of shear capacity in their pier caps due to increase in the required truck loads. Therefore improved understanding of the design methods and performance of these important members is mandatory. This thesis presents the behavior of reinforced concrete hammerhead pier caps using finite element analysis software ABAQUS. The parameters taken in to consideration are material properties (both steel and concrete), shear span to depth ratio (a/d) and flexural reinforcement ratio. Finally, the result obtained from the finite element analysis has been presented and compared with a strut and tie model. The findings of this work shows that as concrete strength increases, both the displacement and maximum principal stress decreased by 49.6% and 28.2% respectively while change in steel grade have no significant effect on the behavior of pier caps. The shear strength predictions using strut and tie models were found to be more conservative compared to the finite element method. The displacement resultant increased from 0.84mm to 12.87mm as the shear span to effective depth ratio increases from 1 to 2.5 however the shear capacity decreased. A comparison of principal stress showed that the solutions based on finite element analysis was 14.45% higher than the strut and tie model. The flexural reinforcement area required using STM method was 14.3% greater than that of sectional design approach.*

Key words: *Hammerhead Pier Caps, Strut and Tie Model, Finite Element Analysis*

1.INTRODUCTION

A pier is a structure which provides the basic function of supporting spans at intermediate points between end supports. Like abutments, piers come in a variety of configurations, shapes, and sizes. The type of pier selected will depend greatly on the form of superstructure present. Hammerhead piers are predominately found in urban settings because they are both attractive and occupy a minimum of space, thereby providing room for underpass traffic. They are also attractive solutions when the structure is located on a skew, thereby creating tight alignment constraints for the underpass traffic. When compared with a column bent pier, the single column hammerhead offers a solution which provides for a more open and free-flowing look, especially in high traffic, multiple structure environments.

Hammerhead piers are typically used where column lengths on multi-column piers will require larger column sizes due to slenderness. They are also an option where stream flow could result in debris build-up between columns of a multi-column pier. Where stream flow is present, hammerhead piers shall be oriented parallel to the direction of flow.

The minimum width and thickness of the pier head or cap depends on the layout and dimensions at the bridge bearings. For hammerhead-type piers, the head is the first item to be designed once the position and magnitude of loads from the super structure are known.

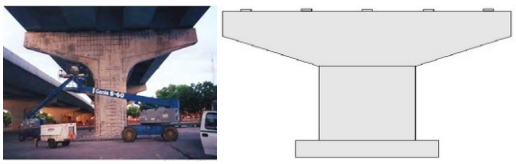

Figure 1.1 Typical hammerhead bridge pier (WisDOT Bridge Manual)

In most instances, hammerhead pier cap can be defined as deep reinforced concrete members and therefore, should be designed using the strut-and-tie modeling approach. However, most bridge engineers do not have a broad knowledge on the STM due to the unfamiliarity with the design procedure. Therefore, it is likely that, with the formulation of a well-defined strut-and-tie modeling procedure, having the awareness will become more comfortable with the design method and therefore,

employ the method more often and consistently. With the rapid economic development of the country in the past decades, a large number of bridges and overpasses were constructed in Ethiopia. Hammerhead piers are widely designed and built for its perfect shapes, convenient construction and covering a minimum space. As a special concrete structure, there is no defined set of laws for designing in current Ethiopian codes. Designers usually analyze pier caps as normal RC bending members. In particular, hammerhead pier caps designed in accordance with Euler-Beam approach may suffer severe cracks after opening to traffic, caused by insufficient strength and inadequate reinforcement detailing. To overcome such problems Strut and tie modeling (STM) is an accepted design method to deal with D-regions since it simplifies the non-linear stresses into a truss model through a series of struts and ties representing the flow of stresses at failure. Therefore, strut and tie model development according to AASHTO LRFD design method was presented for the design of hammerhead bridge pier caps and results were compared with finite element method. The main objective of this study was to compare the behavior of reinforced concrete hammerhead pier caps using finite element method and strut and tie model.

The specific objectives of the study were: -

To study the behavior of hammerhead bridge pier caps and to develop a better understanding of ways designing these important members.

- To conduct a parametric study on the behavior of reinforced concrete pier caps in understanding the actual behavior of the structure on various dimensional and material parameters.
- To compare the flexural reinforcing requirements for typical hammerhead pier caps using both strut-and-tie modeling and standard sectional design practices.

This study focused on the analysis of reinforced concrete hammerhead pier caps for various material grades, shear span to effective depth ratio and longitudinal reinforcement ratio. The analyses were carried out using finite element method and results were compared with strut and tie model. In this study, the analysis was based on the numerical and analytical methods considering the load transferred to the bearing and self-weight of the pier cap.

The significance of this study was summarized as follow;

- It creates good awareness in preparing suitable practical guidelines for designing and simple analysis of hammerhead pier caps.
- To enhance the understanding of the application of the method and it is also useful to be used as reference in the application.
- It is useful to develop Strut and Tie model in analysis and design of reinforced concrete bridge pier caps.

3.RESEARCH METHODOLOGY

3.1 RESEARCH DESIGN

Appropriate analysis and design detailing for reinforced concrete pier caps were required due to the high transferred loads from the girder to the pier cap through bearings. A parametric study on the behavior of pier caps were carried out using strut and tie model by considering different material properties (both steel and concrete), shear span to depth ratio (a/d) and flexural reinforcement ratio. One parameter is considered at a time while the remaining parameters are fixed.

Following the strut and tie model, an analysis will be carried out using finite element method. Identical pier caps with similar geometries, material properties and loading were modeled and analyzed using the general purpose software ABAQUS.

For the design studies, only reaction forces on the bridge bearing pads were considered. The nodal zones are first defined where external loads, like beam reactions, act on the pier cap. It should be noted that the compression struts and tension ties should intersect at the nodal zones and represent the location of the reinforcing pattern.

The solution for the truss forces was accomplished by using an excel template. The truss solution also aid in defining the members that are in tension and compression for complex truss systems. The dimensioning of the compression strut, tension tie, and nodal zones were governed by Article 5.6.3.2 through Article 5.6.3.6 of the AASHTO
LRFD Specifications.

Through parametric studies, it could verify the performance of model in simulating the physical behavior of reinforced concrete pier caps, due to the variation in a certain parameter values. Having modeled the problem of pier caps analysis, the following parameters were used to study the behavior.

Effect of change in geometry: - Pier caps having different shear span to depth ratio (a/d) were considered to study the effect of change in depth on the behavior. The range of shear span to depth ratio was 1 to 2.5.

Parameters	Ranges	
	Minimum	Maximum
Shear span to effective depth ratio ,a/d	1	2.5
Concrete strength (MPa)	C-25	C-45
Steel grades (MPa)	S-300	S-460
Reinforcement ratio (%)	0.40	0.60
Loading condition	Concentrated bearing loads	

Effect of change in concrete strength**:** - Concrete strength varying from C-25 to C-45 was used to conduct a parametric study.

Effect of change in steel grade**:** - the steel grade used for the parametric study varies from S-300 to S-460

Effect of change in reinforcement ratio**:-**The range of reinforcement ratio, ρ, was 0.40% to 0.60%.

Effect of change in analyzing method: - In order to compare the result of finite element analysis with the analytical method which stated in the code provision, the pier caps were analyzed using STM with variable shear span to depth ratio (a/d).

3.2 STUDY VARIABLES

Independent variables:-geometry of the pier cap, material grades, and the loading condition.

Dependent variables:-comparison of the analysis results using strut and tie method and finite element analysis.

3.3 SOURCE OF DATA

The bridge pier cap data used was from Addis Ababa city roads authority (AACRA) supporting a 40m two lane box girder bridge. The dead loads of each component of the bridge super structures required for analysis and design were calculated and transferred to the pier caps following the AASTHO LRFD guidelines. The vehicular live loads transferred to the pier caps were obtained by drawing the influence line of the reaction forces for the 40m continuous span bridge. Finally the loads applied at the bearing points of the pier cap were calculated by using AASHTO load factors.

3.4 DESCRIPTION OF THE MODEL

As an attempt to do a parametric study on the behavior of pier caps, a modeling and stress analysis was carried out. The model used in order to do a parametric study was a pier cap having different shear span to effective depth ratio, concrete strength, and longitudinal reinforcement ratio. The model was first modeled by a finite element method and considering different parameters which affects the behavior of pier caps. The results of finite element analysis were compared with the results obtained by strut-and- tie model.

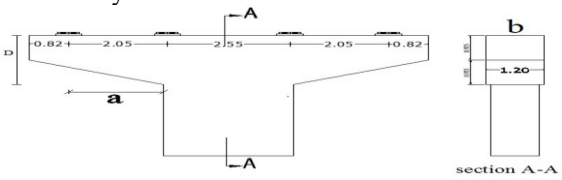

Figure 3.1 Models of pier cap

3.5 FINITE ELEMENT IDEALIZATION

The finite element idealization involves an assemblage of two or three dimensional elements in which the continuum starts with subdivision of the physical system into an assemblage of discrete elements. The accuracy of the solution and efficiency of computational time is governed by the modeling technique and the number of element used. With properly formulated finite elements, the result converges to the exact solution with decreasing element size. Accordingly the larger the number of elements the more accurate the solution obtained.

Compatibility at nodes does not always ensure compatibility across the element boundaries. To avoid such discontinuities, interpolation functions over the element are assumed in such a fashion that the common boundaries will deform together. In static analysis of the finite element method, the state of stress within each element is determined from nodal displacement. This is accomplished using interpolation functions, strain displacement relations and constitutive properties of the material.

The commercial software ABAQUS has been used for modeling the pier caps and doing parametric study. It was chosen in this study because of its popularity and capabilities in handling large range of problems. It is general purpose finite element software solving a wide variety of problems. These problems include static/dynamic problems, structural analysis (both linear and nonlinear), heat transfer, and fluid problems, as well as electromagnetic problems. In general, ABAQUS solution process may be broken into the following three stages.

1) Pre-processing: In pre-processing geometry is divided into number of elements which is connected at discrete points. Some of these nodes will have fixed displacement and other nodes will have loading. This model is time consuming to prepare.

The major steps in pre-processing are:

Define key points/lines/volumes,

Define element type and material/geometric properties, and

1) Mesh lines/areas/volumes as required. The amount of detail required will depend on the dimensionality of the analysis, i.e., 1D, 2D, axisymmetric, and 3D.

2.Analysis

The dataset prepared by the pre-processor is used as input to finite element code itself, which constructs and solves a system of linear or nonlinear algebraic equations. Kij x Uj = Fi, where U and F are displacements and applied force respectively. The formation of the stiffness matrix [K] is dependent on the type of problem. There are large element libraries available in commercial codes. FEA can solve many problems simultaneously that depend upon the code for appropriate type of elements available in library.

The main goal of finite element analysis is to examine how a structure or its component responds to certain loading condition. Specifying the proper loading conditions, is therefore, a key stepping analysis. Assigning loads, constraints, and solving here, it is necessary to specify the loads (point or pressure), constraints (translational and rotational), and finally solve the resulting set of equations. In the solution phase of the analysis, the computer takes over and solves the simultaneous equations that the finite element method generates. The element solution is usually calculated at the elements integration points.

2. Post-processing: Earlier in FEA, the user pores through many codes, listing displacements and stresses at discrete positions in the model. A typical post-processor display overlay colored contours representing stress levels on the model, showing a full-field picture similar to that of experimental results. It shows how the applied loads affect the design, how good finite element mesh is, and so on. Further processing and viewing of the results in this stage one may wish to see (i) lists of nodal displacements, (ii) element forces and moments, (iii) deflection plots etc.

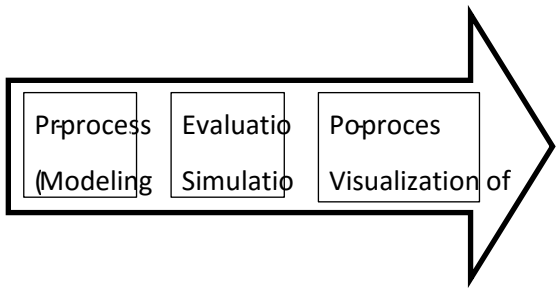

Figure 3.2 Principle steps of ABAQUS

3.6 THREE DIMENSIONAL SOLID ELEMENTS

Generally C3D8R: 8 node linear tetrahedral elements with reduced integration and hourglass control were used to model the concrete. This element has 8 node and 3 DOFs at each node. It has three translational DOFs, i.e. translation in the x, y and z direction. It has 3D 8 nodes structural solid element that exhibits quadratic displacement behavior.

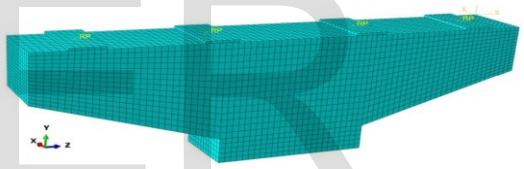

Figure 3.3 Finite element meshes

The quadratic eight node elements shown in Figure 3.3 were adopted to represent concrete. Material property is assumed to be homogenous and isotropic within the material. Linear elastic behavior prior to cracking is assumed in modeling concrete.

3.7 REINFORCEMENT IDEALIZATION

Linear 2-nodes beam elements, B31 are used to model the reinforcement and embedded elements technique is used to embed the reinforcement into the concrete.

In the embedded element technique, the host will be the solid concrete elements while the reinforcement will be the embedded elements. In ABAQUS, the nodes of the embedded elements will lose its translational degrees of freedom in the sense that they are constrained to the translational degrees of freedom of the host elements. However, the embedded

elements are allowed to retain their rotational degrees of freedoms which are not constrained. The number of rotational degrees of freedom allowed in a node of an embedded element is identical to the number of translational degrees of freedom of the host element.

In a three-dimensional model with beam elements in solid elements, since each node at the solid element have three degrees of translational freedom, each beam elements are able to have three rotational degrees of freedom at each node. For the reinforcement, it will retain its own translational degrees of freedom while taking on the interpolated values of the translational degrees of freedom of the host elements.

Beam elements are more suitable than truss elements for modeling of the reinforcement because the former exhibit shear and bending behavior while the latter only resist axial forces. The shear and bending behavior of the beam elements is necessary when refined meshes are used to obtain convergence of results.

3.8 MESHING

After creating of volumes, a finite element analysis requires meshing of the model in which the model is divided into a number of small elements. After loading stresses and strains are calculated at integration points of these small elements.

The mesh size is an important parameter in finite element analysis. In order to arrive at appropriate element size, convergence study with different sizes of mesh is carried out. To obtain more precise and accurate results, the elements size should be small and the element type should contain a large number of nodes.

The negative aspect of this is that the simulation can be time consuming and also the mesh can become too complex to work with. A convergence of results is obtained when an adequate number of elements are used in a model. This is practically achieved when an increase in the mesh density has a negligible effect on the results. By changing the size of the elements used in the model, the optimal mesh size was achieved.

3.9 FINITE ELEMENT MODELING

The FEM software ABAQUS has three concrete material models available for modeling plain or reinforced concrete. They are concrete smeared cracking model, cracking model for concrete and concrete damaged plasticity model (CDP). All three models can be used for plain concrete, even though they are primarily used for reinforced concrete. For concrete in both alternatives, the concrete damage plasticity (CDP) model was used in this study, intended for brittle materials with the possibility of establishing failure criteria by damage parameters.

CDP is suitable for use in which the structure is subjected to monotonic, cyclic and/or dynamic loading under low confining pressures. The concrete behavior is modeled by the theory of isotropic damaged elasticity combined with isotropic compressive and tensile plasticity. The two main failure mechanisms are the compressive failure and the tensile cracking of the concrete.

The concrete was modeled using a 3D deformable tetrahedral homogeneous solid element, due to its ability to better adapt to any member geometry. Although mesh refinement needed is usually smaller if quadratic elements are used, only linear elements were utilized in this study because they are more accurate for plastic behavior. For concrete, AASHTO provides a Poisson‟s ratio of 0.2.

Once done, the results were converted from numerical outputs into visual information accessed in ABAQUS‟s visualization module. From there, the results could easily be read visually at a glance. For example, principal strains were observed directly in the module to study the propagation behavior of cracking over time. Finally, the loaddisplacement curves of the simulation were extracted from the module and exported to an Excel file sheet, where they could easily be compared with the load displacement curves derived from the experiment references.

3.10 CONCEPT OF THE FINITE-ELEMENT METHOD

The finite element method is based on the representation of a body or a structure by an assemblage of subdivisions called finite elements. These elements are considered to be connected at nodes. Displacement functions are chosen to approximate the variation of displacements over each finite element. Polynomials are commonly employed to model these functions. Equilibrium equations for each element are obtained by means of the principle of

minimum potential energy. These equations are formulated for the entire body by combining the equations for the individual elements so that the continuity of displacements is conserved at the nodes. The resulting equations are solved satisfying the boundary conditions in order to obtain the unknown displacements.

The entire procedure of the finite element method involves the following steps:

(1) The given body is subdivided into an equivalent system of finite elements,

(2) A suitable displacement function is chosen,

(3) An element stiffness matrix is derived using variational principle of mechanics such as the principle of minimum potential energy,

(4) The corresponding global stiffness matrix for the entire body is formulated,

(5) The algebraic equations thus obtained are solved to determine unknown displacements and

(6) The element strains and stresses are then computed from the nodal displacements.

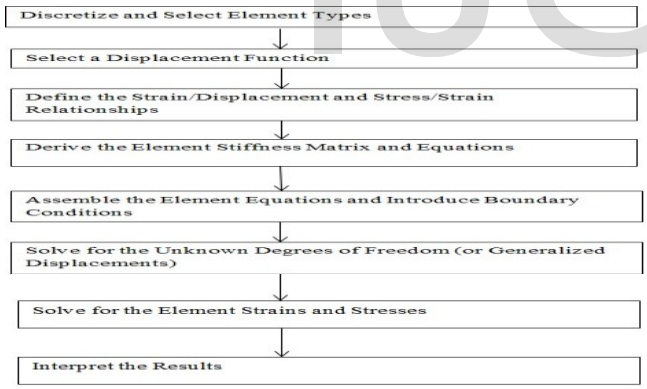

Figure 3.4 Basic steps in setting-up and solving the FEM model.

3.11 BASIC EQUATIONS FROM THE THEORY OF ELASTICITY

Figure 3.4 shows the state of stress in an elemental volume of a body under load. It is defined in terms of three normal stress components σ_x, σ_y and σ_z and three shear stress components τ_{xy}, τ_{yz} and τ_{zx}. The corresponding strain components are three normal strains ε_x, ε_y and ε_z and three shear strains γ_{xy}, γ_{yz} and γ_{zx}. These strain components are related to the displacement components u, v and w at a point as follows:

$$\varepsilon_x = \frac{\partial u}{\partial x} \qquad \gamma_{xy} = \frac{\partial v}{\partial x} + \frac{\partial u}{\partial y}$$

$$\varepsilon_y = \frac{\partial v}{\partial y} \qquad \gamma_{yz} = \frac{\partial v}{\partial z} + \frac{\partial w}{\partial y}$$

$$\varepsilon_z = \frac{\partial w}{\partial z} \qquad \gamma_{zx} = \frac{\partial u}{\partial z} + \frac{\partial w}{\partial x} \quad (1)$$

The relations given in equation (1) are valid in the case of the body experiencing small deformations. If the body undergoes large or finite deformations, higher-order terms must be used. The stress-strain equations for isotropic materials may be written in terms of the Young‟s modulus and Poisson‟s ratio as follows:

$$\sigma_x = \frac{E}{1-\upsilon^2}[\varepsilon_x + \upsilon(\varepsilon_y + \varepsilon_z)]$$

$$\sigma_y = \frac{E}{1-\upsilon^2}[\varepsilon_y + \upsilon(\varepsilon_x + \varepsilon_z)]$$

$$\sigma_z = \frac{E}{1-\upsilon^2}[\varepsilon_z + \upsilon(\varepsilon_y + \varepsilon_x)]$$

$$\tau_{xy} = G\gamma_{xy}, \tau_{yz} = G\gamma_{yz}, \tau_{zx} = G\gamma_{zx} \quad (2)$$

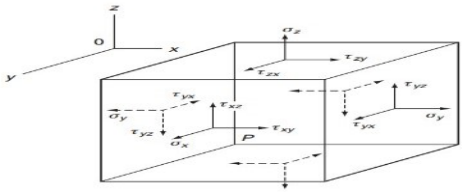

Figure 3.5 State of stress in an elemental volume (Gerard P. and Nigel.H, 2008)

Plane stress

When the elastic body is very thin and there are no loads applied in the direction parallel to the thickness, the state of stress in the body is said to be plane stress. The plate is subjected to in plane loading. In this case, $\sigma_z = \tau_{yz} = \tau_{zx} = 0$ and the constitutive relation for an isotropic continuum is expressed as:

$$\begin{bmatrix}\sigma_x\\ \sigma_y\\ \tau_{xy}\end{bmatrix} = \frac{E}{1-\upsilon^2}\begin{bmatrix}1 & \upsilon & 0\\ \upsilon & 1 & 0\\ 0 & 0 & \frac{1-\upsilon}{2}\end{bmatrix}\begin{bmatrix}\varepsilon_x\\ \varepsilon_y\\ \gamma_{xy}\end{bmatrix} \quad (3)$$

Plane strain

The state of plane strain occurs in members that are not free to expand in the direction perpendicular to the plane of the applied loads. Examples of some plane strain problems are retaining walls, dams, long cylinder, tunnels, etc. In these problems $\varepsilon_x, \gamma_{yz}$ and γ_{zx} will vanish and hence: $\sigma_z = \upsilon(\sigma_x + \sigma_y)$

The constitutive relations for an isotropic material are written as:

$$\begin{bmatrix}\sigma_x\\ \sigma_y\\ \tau_{xy}\end{bmatrix} = \frac{E}{(1-\upsilon)(1-2\upsilon)}\begin{bmatrix}(1-\upsilon) & \upsilon & 0\\ \upsilon & (1-\upsilon) & 0\\ 0 & 0 & \frac{1-2\upsilon}{2}\end{bmatrix}\begin{bmatrix}\varepsilon_x\\ \varepsilon_y\\ \gamma_{xy}\end{bmatrix} \quad (4)$$

3.12 CHOICE OF DISPLACEMENT FUNCTION

The selection of a suitable displacement function is an important step in finite-element analysis, since it defines the performance of the element in the analysis. A polynomial is the most common form of displacement function. Mathematics of polynomials are easy to handle in formulating the desired equations for various elements and convenient in digital computation. The degree of approximation is governed by the stage at which the function is truncated. Solutions closer to exact solutions can be obtained by including more number of terms. The polynomials are of the general form:

$$w(x) = a_1 + a_2x + a_3x^2 + \cdots a_{n+1}x^n \quad (5)$$

The coefficients a are known as generalized displacement amplitudes. The general polynomial form for a two-dimensional problem can be given as:

$$u(x,y) = a_1 + a_2x + a_3y + a_4x^2 + a_5xy + a_6y^2 + \cdots + a_my^n$$

$$v(x,y) = a_{m+1} + a_{m+2}x + a_{m+3}y + a_{m+4}x^2 + a_{m+5}xy + a_{m+6}y^2 + \cdots + a_{2m}y^n \quad (6)$$

These polynomials can be condensed at any desired degree to give constant, linear, quadratic or higher-order functions. For example, a linear model in the case of a two dimensional problem can be given as:

$$u = a_1 + a_2x + a_3y$$

$$v = a_4 + a_5x + a_6y \quad (7)$$

A quadratic function is given by:

$$u = a_1 + a_2x + a_3y + a_4x^2 + a_5xy + a_6y^2$$

$$v = a_7 + a_8x + a_9y + a_{10}x^2 + a_{11}xy + a_{12}y^2 \quad (8)$$

3.13 FORMULATION OF STIFFNESS MATRIX

It is possible to obtain all the strains and stresses within the element and to formulate the stiffness matrix and a consistent load matrix once the displacement function has been determined. This consistent load matrix represents the equivalent nodal forces which replace the action of external distributed loads. The displacement function may be written in the form:

$$\{f\} = [P]\{A\} \quad (9)$$

In which $\{f\}$ may have two components {u, v}, [P] is a function of x and y only, and {A} is the vector of undetermined constants. If equation (9) is applied repeatedly to the nodes of the element one after the other, we obtain a set of equations of the form:

$$[d] = \{C\}[A], \quad (10)$$

in which d is the nodal parameter and [C] is the relevant nodal coordinates. The undetermined constants {A} can be expressed in terms of the nodal parameters $\{d\}$ as:

$$\{A\} = [C]^{-1}[d] \quad (11)$$

Substituting equation (11) in to equation (9)

$$\{f\} = [P][C]^{-1}[d] \quad (12)$$

Constructing the displacement function directly in terms of the nodal parameters one obtains:

$$\{f\} = [N]\{d\} \quad (13)$$

Where [N] is a shape function written as function of both (x, y) and given by:

$$[N] = [P][C]^{-1} \quad (14)$$

The various components of strain can be obtained by appropriate differentiation of the displacement function. Thus:

$$\{\varepsilon\} = [B]\{d\} \quad (15)$$

Where $[B]$ is derived by differentiating appropriately the elements of [N] with respect to x and y. The stresses {σ} in a linearly elastic element are given by the product of the strain and a symmetrical elasticity matrix [D]. Thus:

{σ}= [D]{ε} or {σ} = [D][B]{d} (16) The elasticity matrix [D] in case of isotropic materials, for plane stress

$$[D] = \frac{E}{1-\upsilon^2}\begin{Bmatrix} 1 & \upsilon & 0 \\ \upsilon & 1 & 0 \\ 0 & 0 & \frac{1-\upsilon}{2} \end{Bmatrix} \quad (17)$$

And for plane strain case

$$[D] = \frac{E}{(1+\upsilon)(1-2\upsilon)}\begin{Bmatrix} 1-\upsilon & \upsilon & 0 \\ \upsilon & 1-\upsilon & 0 \\ 0 & 0 & \frac{1-2\upsilon}{2} \end{Bmatrix}$$

The stiffness and the consistent load matrices of an element can be obtained using the principle of minimum total potential energy. The potential energy of the external load in the deformed configuration of the element is written as:

$$W = -\{d\}^T\{d\} - \int\{f\}^T\{q\}da \quad (19)$$

In equation (19), $\{d\}$ represents concentrated loads at nodes and {q} the distributed loads per unit area. Substituting for $\{f^T\}$ from equation (19) one obtains:

$$W = -\{d\}^T\{d\} - \{d\}^T\int\{N\}^T\{q\}\,da$$

$$U = \frac{1}{2}\int\{\varepsilon\}^T\{\sigma\}dv \quad (20)$$

Note that the integral is taken over the area a of the element. The strain energy of the element integrated over the entire volume, v, is given as follows. Substituting for $\{\varepsilon\}$ and $\{\sigma\}$ from equations (15) and (16) respectively.

$$U = \frac{1}{2}\{d\}^T(\int[B]^T[D][B]\,dv)\{d\} \quad (21)$$

The total potential energy of the element is

$$V = U + W \text{ Or}$$

$$V = \frac{1}{2}\{d\}^T(\int[B]^T[D][B]dv)\{d\} - \{d\}^T\{Q^*\} - \{d\}^T\int[N]^T\{$$

(22)

Using the principle of minimum total potential energy, we obtain:

$$(\int[B]^T[D][B]\,dv)\{d\} = \{d\} + \int[N]^T\{q\}\,da$$

Or$[K]\{d\} = \{F^*\}$, Where: [K] =$\int[B]^T[D][B]dv$

(23) Coordinate transformation

= x (s, t) s = s (x, y)

= y (s, t) t = t (x, y)

Jacobian matrix

$$\begin{Bmatrix} \frac{\partial x}{\partial s} & \frac{\partial y}{\partial s} \\ \frac{\partial x}{\partial t} & \frac{\partial y}{\partial t} \end{Bmatrix} = \frac{1}{8}(x_c)^T\begin{Bmatrix} 0 & 1-t & t-s & s-1 \\ t-1 & 0 & s+1 & -s-t \\ s-t & -s-1 & o & t+1 \\ 1-s & s+1 & -t-1 & 0 \end{Bmatrix}\{y_c\}$$

[J]=

$$\{x_c\} = \begin{Bmatrix} x_1 \\ x_2 \\ x_3 \\ x_4 \end{Bmatrix}, \{y_c\} = \begin{Bmatrix} y_1 \\ y_2 \\ y_3 \\ y_4 \end{Bmatrix}$$

Where,

$$[\mathrm{B(s,t)}] = \frac{1}{|J|}\{B_1 \quad B_2 \quad B_3 \quad B_4\}$$

$$[B_1] = \begin{Bmatrix} a(N_{i,s}) - b(N_{i,t}) & 0 \\ 0 & c(N_{i,t}) - d(N_{i,s}) \\ c(N_{i,t}) - d(N_{i,s}) & a(N_{i,s}) - b(N_{i,t}) \end{Bmatrix}$$

Where

$$N_{1,s} = \frac{\partial N_1}{\partial s} = \frac{(t-1)}{4} \qquad N_{1,t} = \frac{\partial N_1}{\partial t} = \frac{(s-1)}{4}$$

$$N_{2,s} = \frac{\partial N_2}{\partial s} = \frac{(1-t)}{4} \qquad N_{2,t} = \frac{\partial N_2}{\partial t} = \frac{-(s+1)}{4}$$

$$N_{3,s} = \frac{\partial N_3}{\partial s} = \frac{(t+1)}{4} \qquad N_{3,t} = \frac{\partial N_3}{\partial t} = \frac{(s+1)}{4}$$

$$N_{4,s} = \frac{\partial N_4}{\partial s} = \frac{-(t-1)}{4} \qquad N_{4,t} = \frac{\partial N_4}{\partial t} = \frac{(1-s)}{4}$$

$$a = \tfrac{1}{4}[y_1(S-1) + y_2(-S-1) + y_3(S+1) + y_4(1-S)]$$

$$b = \tfrac{1}{4}[y_1(t-1) + y_2(1-t) + y_3(t+1) + y_4(-1-t)]$$

$$c = \tfrac{1}{4}[x_1(t-1) + x_2(1-t) + x_3(t+1) + x_4(-1-t)]$$

$$d = \frac{1}{4}[x_1(S-1) + x_2(-S-1) + x_3(S+1) + x_4(1-S)]$$

Addition of these element matrices in accordance with the nodal numbering of each element yields the stiffness matrix for the entire structure [K].

3.14 SCOPE AND LIMITATIONS OF THE MODEL

This thesis work focused on the analysis of reinforced concrete pier caps. The analysis was carried out using finite element software ABAQUS with its implemented features such as the material models for steel and concrete. The purpose of this study was to study the behavior of hammerhead bridge pier caps and to develop a better understanding ways of designing these important members. This significant perception leads to creating a good awareness in preparing suitable practical guidelines for designing and simple analysis of pier caps. Modeling discontinuous regions in exact way is not an easy task; so that simplifications are required but such simplifications must not affect the results from the simulation. The most important limitation is that the concrete is modeled as a linear elastic material, which means that redistribution of stress due to cracks in the concrete is not considered in the model. The other important assumption in finite element analysis was that the material is isotropic and homogeneous.

3.15 DATA PRESENTATION AND ANALYSIS

Analysis results obtained using strut and tie model and finite element analysis were compared to each other and presented graphically. The following out puts were presented in this thesis work.

- The effect of change in material strength on the response of pier caps
- The variation of shear with change in shear span to depth ratio
- The effect of changing longitudinal reinforcement ratio on the behavior of pier caps
- The differences between analysis results using the two methods were presented
- Finally conclusions were made and recommendations for future studies were forwarded.

4.RESULTS AND DISCUSSION

AASHTO LRFD specifications recommend the use of STM for the design of Dregions (AASHTO 5.6.3.1) and pier caps tend to be composed of entirely or mostly D-regions due to their large depths and the frequent application of concentrated loads from the girders they support. Figure 4.5 shows a hammerhead pier cap with relatively long and slender cantilevered portions sticking out from the column. The compressive struts in the STM model generally represent the elastic stress trajectories in the cap. Ties in the model are the solid lines which include a series of longitudinal ties across the top of the cap and vertical ties. A bar size is usually assumed for the shear ties and the required spacing is calculated for each band.

4.1 PIER CAP DESIGN EXAMPLE

The bridge pier cap designed in this section is from Addis Ababa city roads authority (AACRA) supporting a 40m two lane box girder bridge. Bridge material properties and loading calculations and the procedure for the strut and tie modeling of the pier cap is demonstrated in this section

Table 4.1 Material properties

Loading calculations

Table 4.2 Dead loads

Point of loading	Super structural dead load reaction	Reaction from wearing surface
From exterior girders	R_{DCE} = 918.18 KN	R_{DWE} = 79.09 KN
From interior girders	R_{DCI} =818.89 KN	R_{DWI} = 97.01 KN

Vehicle live loads acting on the bridge deck are carried through the girders onto the bearing surface of the pier. The truck or tandem loads transferred to the bearings was calculated by drawing the influence line of the reaction forces for the 40m continuous span bridge.

Figure 4.1 Influence line for the maximum reaction on the pier

The maximum reaction on the pier due to truck load plus lane load adjusted by importance factor and reaction factor is given in table below.

Table 4.3 vehicular live loads

	Truck load	Lane load	(Truck +lane)adjusted by Im & Rf
Exterior girder	313.41 KN	145.29 KN	454.197KN
Interior girder	313.41 KN	178.23 KN	471.89 KN

Bridge pier total bearing loads

The super structural dead loads, dead load due to wearing surface and vehicular live loads are combined together using the load combination provided on AASHTO guideline.

Material properties	Values
Concrete grade	C-30, f_{ck}=25Mpa, v = 0.2
Concrete density	24 KN/m^3
Steel reinforcement	S-400, v =0.3 , E = 200Gpa

AASHTO load factors in Table 4-4 were used to calculate the total factored girder reactions acting at each bearing point of the pier cap.

Table 4.4 Factored girder reactions acting at each bearing point

	Super structure dead load(DC)	Dead load due to wearing surface (DW)	Vehicular live load(LL)	Total Bearing load =1.25(DC) +1.5(DW) +1.75(LL)
Exterior girder	918.18 KN	79.09 KN	454.197 KN	2061.2 KN
Interior girder	818.89 KN	97.01 KN	471.89 KN	1995 KN

In addition to these bearing loads, the pier cap is subjected to its own self weight and is added to the bearing loads for the design. The self-weight calculation is shown here along with the resulting force distribution along the pier cap.

Force from self-weight = (width) x (height) x (unit weight of concrete) x (load factor)

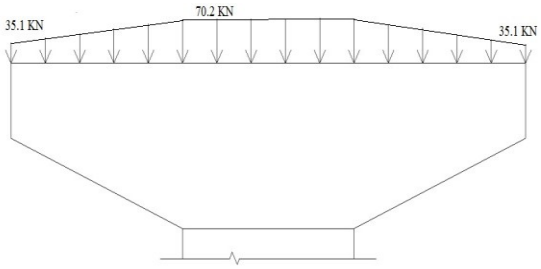

Figure 4.2 Bridge pier cap self-weight

The self-weight of the pier cap is applied as resultant forces acting on the four bearing points as shown in Table 4.5. These forces are added to the applied loads from the girders Table 4.4. Figure 4-3 shows the final

loading that is used for the STM design. Table 4.5 Self-Weight Resultant Forces

Bearing	1	2	3	4
Force in KN	85.69	168.26	168.26	85.69

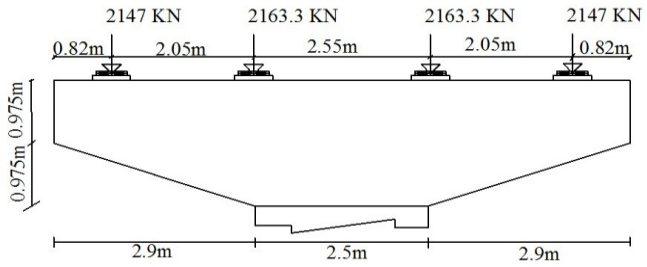

Figure 4.3 Pier cap final loading

AASHTO STM Design

1. Delineate D-regions from B-regions

The entire pier cap is considered to be in the D-region since the smallest beam depth dimension is 0.975m. And the distance between the bearing concentrated loads is 2.05, which is almost close to 2(d) = 1.95m. Even if part of the cap were to be considered as a B-region, it would still be reasonable to do the entire design with STM.

2. Determine the Boundary Conditions on the D-region

To generalize the pier cap as a truss, the column under it is considered as two compressive struts. These struts are resisted by two supports to prevent displacement in the y-direction only.

3. Visualize/ sketch the flow of stresses

Plots of principal compressive and tensile stress vectors aided the development of a strut-andtie model.

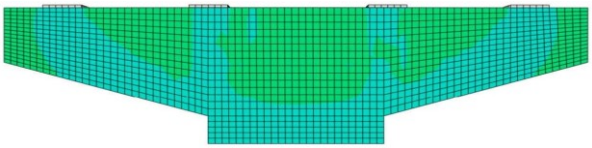

Figure 4.4 stress distribution contour

4. Develop a STM that is compatible with the flow of forces.

The model used should realistically represent the distribution of stresses from figure 4.4. The width of the column struts are calculated based on the percentage of the load they carry to total load in the column. And then these strut dimensions are used in the creation of the truss model.

Column strut width = $\frac{Forces\ supplied\ by\ one\ strut}{\sum Forces} * column\ width$

$= \frac{2147+2163.3}{2(2147+2163.3)} * 2.5m = 1.25m$

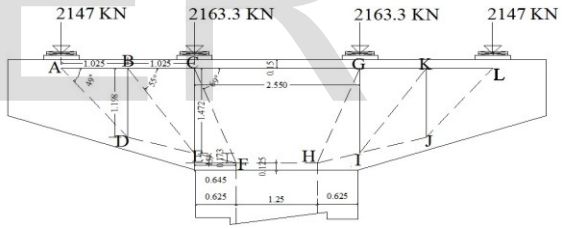

Figure 4.5 Strut and tie model

Dimensioning the truss model

It was assumed that the horizontal tie spanning the top of the pier cap should be placed at 0.15m (150mm) from the top edge of the cap. This accounts (50mm cover +shear ties + two layers of longitudinal ties) that is expected based on sectional analysis

Depth of pier cap D = 1.95m Effective depth d=D-cover-24(stirrup)-32(bar)-20(half bar spacing) = 1950 -(50+24+32+20)=1824mm

$M_u = 2147 * 2.695 + 2163.3 * 0.65 = 7192.31\ KN - M$

$$M_u = \emptyset M_n = \emptyset * 0.85 * f_{ck*} ab \left(d - \frac{a}{2}\right) \quad where\ \emptyset = 0.7$$

$$7192.31 * 10^6 Nmm = 0.7 * 0.85 * 25 * 1200 * a \left(1824 - \frac{a}{2}\right)$$

Solving for a

$gives\ a = 236mm\ use\ a \cong 250mm$

Therefore the line representing the centerline of the bottom struts will be placed at 125mm from the bottom edge of the pier cap.

5. Calculate forces in struts and ties.

Since the model geometry can easily be changed and member forces recalculated if necessary Excel templates was used to compute the forces in truss members. However, it is also a good idea to check some of the members by hand calculations to verify that the model is set up properly. All member forces are shown in Table 4.6.

Table 4.6 Strut and tie member forces

Members	Forces (KN)	Type
AB & KL	1866.359	Tension
AD & LJ	-2844.8	Compression
BD & KJ	1646.911	Tension
BC & GK	3019.538	Tension
DE & IJ	-1932.2	Compression
BE & KI	-2010.51	Compression
CE & GI	1337.917	Tension
CF & HG	-3750.31	Compression
EF & HI	-3126.06	Compression
FH	-4363.53	Compression
CG	4363.529	Tension

Size the area of ties.

For ties AB and KL

The factored resistance of struts and ties shall be taken as that of axially loaded components

$$P_r = \emptyset P_n \quad \ldots\ldots\ldots\ldots\ ASSTHO\ 5.6.3.2.1$$

Where P_n = nominal resistance of struts or ties (N)

$\emptyset$ = Resistance factor for tension or compression specified in Article 5.5.4.2

$\emptyset = 0.9$ For tension in reinforced concrete

$\emptyset = 0.7$ For compression in strut and tie models

$P_n = f_y A_{st}$ Assume $f_y = 400\ Mpa$

$\emptyset f_y A_{st} \geq P_u$

$$A_{st} \geq \frac{P_u}{\emptyset f_y} = \frac{1866.359*10^3\ N}{0.9*400\ ^N/_{mm^2}} = 5184.33\ mm^2$$

Using $\phi_{32}\ bars$ with ^{2}

$$a_{st} = \frac{\pi*32}{4} = 804.2\ mm^2$$

$$\#32\ \text{bars required} = \frac{A_{st}}{a_{st}} = 6.45\ use\ 7\ bars\ in\ one\ rows$$

$$A_{st\ provided} = \frac{7*\pi*32^2}{4} = 5629.73\ mm^2$$

For ties BC & GK

$$A_{st} = \frac{3019.538*10^3\ N}{0.9*400\ ^N/_{mm^2}} = 8387.61\ mm^2$$

$$\#32\ \text{bars required} = \frac{A_{st}}{a_{st}} = 10.43\ use\ 11\ bars\ in\ two\ rows$$

$$A_{st\ provided} = \frac{11*\pi*32^2}{4} = 8846.72\ mm^2$$

For tie CG

$$A_{st} = \frac{4363.529*10^3\ N}{0.9*400\ ^N/_{mm^2}} = 12120.91\ mm^2$$

$$\#32\ \text{bars required} = \frac{A_{st}}{a_{st}} = 15.07\ use\ 16\ bars\ in\ two\ rows$$

$$A_{st\ provided} = \frac{16*\pi*32^2}{4} = 12867.96\ mm^2$$

Check the assumed location of the tie centroid for two rows of bars 50(clear cover) + 24(dia. of stirrup) + 32(dia. of bar) + 20(half of bar spacing) = 50 + 24 + 32 + 20 = 126mm < 150mm so the assumed location is ok! Check horizontal spacing of longitudinal steel

$$\frac{cap\ width - 2(clear cover) - 4(dia.\ of\ stirrups) - 8(dia.of\ bars)}{7\ spaces}$$

$= \frac{1200-2*50-4*24-8*32}{7} = 106.9\ mm > 1.5\ d_b = 48\ mm$

Hence horizontal spacing of 8 bars in two rows is ok!

Provide additional crack control reinforcement

Shear reinforcement (AASTHO 5.6.3.6) LRFD 2012

Check minimum reinforcement (assume ϕ_{24}bars to use)

The minimum vertical web reinforcement is given by

$$A_v \geq 0.003bs_v \Rightarrow s_v = \frac{A_v}{0.003b} = \frac{2*\pi*24^2}{0.003*4*1200} = 251.33mm\ use\ s_v$$

$$= 250mm$$

$$A_{st} = 0.003bs_v = 900mm^2 < \frac{4*\pi*24^2}{4} = 1810mm^2$$

Use ϕ_{24} bars @ 250mm c/c vertical web reinforcements

The minimum horizontal web reinforcement is given by

$$A_h \geq 0.003bs_h \Rightarrow s_h = \frac{A_h}{0.003b} = \frac{2*\pi*24^2}{0.003*4*1200} =$$

$$use\ s_h = 250mm$$

Provide ϕ_{24} bars @ 250mm c/c horizontal web reinforcements

$A_h = A_v = 0.003*1200*250 = 900mm^2 < 2*452.$
…ok!

7. Check stresses in the nodal zones and struts.

Strut FH: $P_u = 4363.53\ KN$

Since there are no ties designed to run through these struts ε_1 can be taken as zero.

$$fcu = \frac{fck}{0.8+170*\varepsilon 1} \leq 0.85*fck$$

$$f_{cu} = \frac{25}{0.8} = 31.25 > 0.85*25 = 21.25\ Mpa$$

$$\emptyset P_n = \emptyset f_{cu} A_{cs} \geq P_u = 4363.53\ KN\ but\ A_{cs} = 300*1200 =$$

$$= 0.7*21.25*0.36*1000 = 5355.00$$

$$KN > 4363.53\ KN \quad ok!$$

Nodal zone C and G

The bearing pad area is 550 mm x 550mm

The nodes are considered as C-T-T nodes with $\beta_n = 0.65$

Therefore, the limiting compressive stress in the concrete nodal zone is taken as

$f_{ce} = 0.65*\emptyset f_{ck} = 0.65*0.75*25 =$ 12.19
$Mpa\ and\ P_u = 2163.3KN$

$A_{ce} = \frac{P_u}{f_{ce}} = \frac{2163.3*10^3\ N}{12.19\frac{N}{mm^2}} = 177501.5\ mm^2 < 302500mm^2$ *ok!*

Strut CF

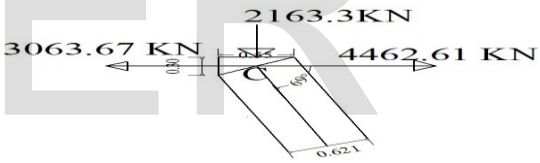

Figure 4.6 Node C

The angle between the strut and the adjoining tie is 69°

Width of strut CF = $550*sin(69) + 300*\cos(69) =$ 620.9796mm = 0.621m

Force in strut CF = 3750.311 KN

$$fcu = \frac{fck}{0.8+170*\varepsilon 1} \leq 0.85*fck$$

$$\varepsilon 1 = \varepsilon s + (\varepsilon s + 0.002)\,cot^2\,\alpha s$$

The strains in the tie (ε_s) can be taken as the average of the strains in tie BC and CG Tie BC

$$f_s = \frac{A_{st\ req}}{A_{st\ prov}} * f_y = \frac{8387.61}{8846.72} * 400 = 379.24\ Mpa$$

ε_s in tie BC $= \frac{f_s}{E} = \frac{379.24\ Mpa}{210\ Gpa} = 0.00190$

Tie CG

$$f_s = \frac{A_{st\ req}}{A_{st\ prov}} * f_y = \frac{12120.91}{12867.96} * 400 = 376.78\ Mpa$$

ε_s in tie CG $= \frac{f_s}{E} = \frac{385.33\ Mpa}{210\ Gpa} = 0.00188$

Average strain in ties BC & CG ε_s= 0.00189

$$\varepsilon_1 = 0.00189 + (0.00189 + 0.002)\,cot^2\,69 = 0.00246$$

$f_{cu} = \frac{25}{0.8+170*0.00246} \leq 0.85 * 25 \Rightarrow 20.51 < 21.25 \quad \therefore use\ f_{cu} = 20.51\ Mpa$

$A_{cs} = 0.621 * 1200 = 45175.5mm^2 = 0.745175\ m^2$

$\emptyset P_n = \emptyset f_{cu} A_{cs} = 0.7 * 20.51 * 0.745175 * 1000 = 10699.93KN > 3750.31\ \text{KN} \quad ok!$

Nodal zone A and L

Considered as C-C-T node, $\beta_n = 0.75$ and $P_u = 2147KN$

$f_{ce} = 0.75\emptyset f_{ck} = 0.75 * 0.75 * 25 = 14.06Mpa$

$A_{cs} = \frac{2147*10^3}{14.06} = 152675.56mm^2$

Strut AD

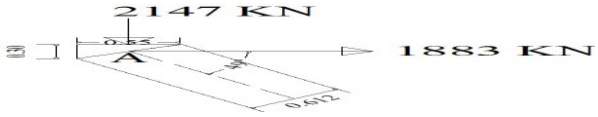

Figure 4.7 Node A

The angle between the strut and the adjoining tie is 49°

Width of strut AD = $550 * sin(49) + 300 * \cos(49) = 611.9\text{mm} = 0.612$ m Force in strut AD = 2844.8KN

Tie AB

$f_s = \frac{A_{st\,req}}{A_{st\,prov}} * f_y = \frac{5184.33}{5629.73} * 400 = 368.3534\ Mpa$

ε_s in tie AB = $\frac{f_s}{E} = \frac{368.3534\ Mpa}{210\ Gpa} = 0.001842$

$\varepsilon_1 = 0.001842 + (0.001842 + 0.002)\ cot^2 49 = 0.00474$

$A_{cs} = 611.9 * 1200 = 0.73428m^2$

$f_{cu} = \frac{25}{0.8+170*0.00433} \leq 0.85 * 25 \Rightarrow 15.56 < 20.4 \quad \therefore use\ f$

$\emptyset P_n = \emptyset f_{cu} A_{cs} = 0.7 * 15.65 * 0.73428 * 1000 = 7998.09KN > 2844.8\ \text{KN} \quad ok!$

9. Provide adequate anchorage for steel tie reinforcement

According to AASTHO LRFD 5.11.2.4, for longitudinal steel, anchorage will be provided by 90° hooks.

The length of the hook should be at least $12d_b$= 12*32= 384mm

Provide 400mm development length and a fillet radius of $4d_b$= 4*32 = 128mm

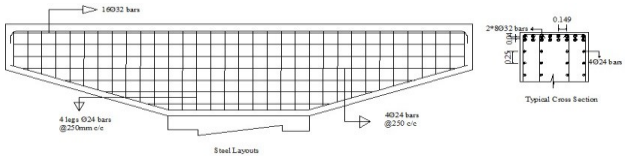

Figure 4.8 Detail of the Pier Cap

Check for minimum transverse reinforcement

A minimum amount of transverse reinforcement is required to restrain the growth of diagonal cracking and to increase the ductility of the section. a larger amount of transverse reinforcement is required to control cracking as the concrete strength is increased.

$A_v \geq 0.083\sqrt{f'c} * \frac{b_v s}{f_y}$

AASHTO 5.8.2.5

Where s- spacing of transverse reinforcement (mm)

A_v –Area of transverse reinforcement with in the distance„s" (mm) f_y –Yield strength of transverse reinforcement

b_v –Width of web adjusted for the presence of ducts as specified in Article 5.8.2.9(mm)

$A_v \geq 0.083\sqrt{25} * \frac{1200*250}{400} = 1809.557\ mm^2 > 311.25\ mm^2$

Check for maximum spacing of transverse reinforcement (AASTHO 5.8.2.7)

The shear stress on the concrete shall be determined as

$v_u = \frac{V_u}{\phi b_v d_v} = \frac{4310.3*10^3}{0.9*1200*1530} = 2.46\frac{N}{mm^2}$ Where d_v is the larger of 0.9d or 0.72h

$v_u < 0.125f'c \Rightarrow 2.46\frac{N}{mm^2} < 0.125 * 25 = 3.1253\frac{N}{mm^2}$

Ok!

$\therefore\ S_{max} = 0.8d_v = 0.8 * 1530mm = 1224mm > 600mm$

Sections that are highly stressed in shear require more closely spaced reinforcement to provide crack control. Hence the maximum spacing permitted is 600mm.

Nominal shear resistance of the sections (V_n) be determined as the lesser of

$$or \quad V_n = \begin{cases} V_c + V_s \\ 0.25f'_c d_v b_v \end{cases}$$ Where

$V_c = 0.083\beta\sqrt{f'c} * b_v d_v$

$$V_s = \frac{A_v f_y d_v (cot\theta + \cot\alpha)\sin\alpha}{S}$$

$$V_s = \frac{A_v f_y d_v (cot\theta)}{S} \quad for\ \alpha = 90°$$

Since the reinforcement provided is greater than the minimum amount of reinforcement required (AASTHO) the following values may be used for $\theta\ and\ \beta.$

i.e. $\theta = 45°\ and\ \beta = 2$

$V_c = 0.083 * 2 * \sqrt{25} * 1200 * 1530 * 10^{-3} = 1613.52$

$V_s = \frac{1963.5 * 400 * 1530\ (\cot 45)}{250} * 10^{-3} =$ 5089.38 KN

$V_n = (1613.52\ KN + 5089.38\ \text{KN}) = 6702.9 KN$

$\emptyset V_n = 0.9 * 6702.9 = 6032.6 KN \geq V_u = 4310.3\ KN$

The shear resistance of a pier cap with shear span to depth ratio $(\frac{a}{d})$ of 1.5= 6032.6 KN.

Design using conventional approach

The maximum moment occurs at the face the column

$M = 2147 * 2.075 + 2163.3 * 0.025 = 4509.11$ KN-m

$d_{provided} = 1900 - (cc + \emptyset_{stirrup} + \frac{\emptyset_{rebar}}{2})$

$= 1900 - (50 + 24 + 32 + 16) = 1778\ mm$

The maximum reinforcement is limited by the ductility requirement which is given by AASHTO art. 5.7.3.31

For $f'c > 28\ Mpa, \beta_1$ shall be reduced at a rate of 0.05 for each of the 7 Mpa of strength in excess of 28 Mpa except that β_1 shall not be taken to be less than 0.65.

$\frac{c}{d} \leq 0.42$ But $a = \beta_1 * c$, where

$\beta_1 = 0.85 for\ f'c \leq 28\ Mpa$

In this case $f'c = 25\ Mpa$

$\frac{c}{d} \leq 0.42$, $\frac{a}{d_e \beta_1} \leq 0.42 \Rightarrow a = 0.42 d_e \beta_1$

$M = 0.85 * \emptyset f'c * b * a(d - \frac{a}{2})$

$= 0.85 * 0.9 * 25 * 1200 * 0.357d\left(d - \frac{0.357d}{2}\right) = 673$

$6730.67d^2 = 4509.11 \Rightarrow d = 818.5\ mm < d_{provided}$

Therefore $a = 0.85 * 0.42 * 1778\ mm = 634.75\ mm$

$\rho = \frac{M_u}{\emptyset f_y b d(d - \frac{a}{2})} = \frac{4509.11 * 10^6}{0.9 * 400 * 1200 * 1778(1778 -}$

$\rho_{min} = \frac{0.03 f'c}{f_y} = 0.03 * \frac{25}{400} = 0.00187 < \rho$

Ok!

$A_s = \rho b d = 0.00513 * 1200mm * 1778mm = 10945$

Provide $\emptyset_{32}\ bars$

$\#\ 32\ bars = \frac{A_s}{a_s} = \frac{10945.368}{\pi * \frac{32^2}{4}} = 13.6 \cong 14\ bars\ in\ two\ rows$

$A_{s\ provided} = 11259.5 mm^2$

Spacing $= \frac{b - 2(cc + 2 * \emptyset_{stirrup} + \frac{\emptyset}{2})}{5} = \frac{1200 - 2 * (25 + 2 * 24 + 16)}{5} = 204.4\ mm$

Provide 14 $\emptyset_{32}\ bars\ @200\ c/c\ in\ two\ rows$

The difference of flexural reinforcement area required using STM method and sectional design approach is 14.3%

4.2 VALIDATION OF FINITE ELEMENT MODEL

Verification and validation of FE codes is necessary before the FE code is used for analysis and simulation for any topics of interest. This is to impart greater confidence in the FE codes used and the results obtained.

Validation on the other hand attempts to assess the accuracy of the computational solution to the real world or experimental data. There is no reason to believe that the experimental data will be more accurate than the computational solution but only that the experimental data is the closest benchmarks for validation.

The experimental and numerical load-deflection curve for the pier cap is shown in Fig. 4.10. It shows that the FEM model predicts the load-deflection curve for pier cap to be slightly stiffer compared to the experimental results.. The experimental loaddeflection curve shows that the pier cap was failed at an ultimate load of 2912.5 KN. The same load and geometry is used for finite element simulation. It was found that the maximum deflection at failure was 6.98% higher in the FEM model (15.9 mm) compared to the experimental results (14.79 mm).

As shown from Figure 4.9, the pier cap was loaded on the top and two supports form the bottom. Identical loading, geometry and boundary conditions were used in the finite element model assuming the support plates as a rigid body.

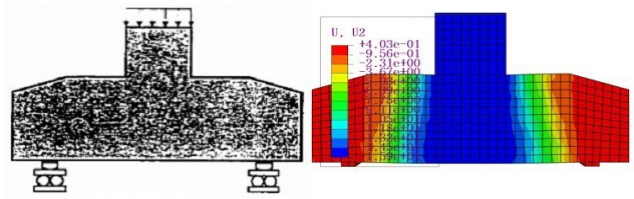

Test set up Finite element model

Figure 4.9 Experimental set up vs. Finite element model

The difference in the FEM and the experimental results could be due to the perfect bond assumption between concrete and steel in addition to the uncertainty involved in the actual material strength.

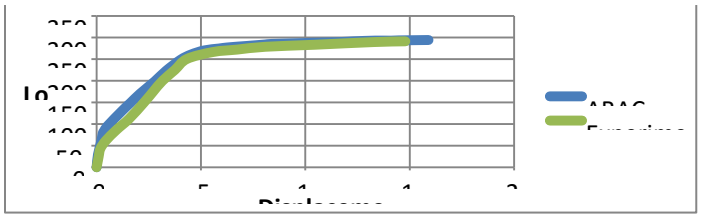

Figure 4.10 Comparison of load vs. displacement curve using Experiment and FEM.

In general, the load-deflection curve from the experiment and the FEM analysis were in good agreement. This indicates that the constitutive models used for concrete and steel are able to capture the behavior of pier cap accurately.

Modeling of the pier cap was undertaken as illustrated in chapter three. After preparing the model that depicts the pier caps property, meshing of the elements was undertaken and static analysis was conducted. The material properties used for the model were described in chapter three.

This section presents the results obtained from the parametric study. By examining the effects of different parameters on the model, a better understanding of how each component of the model contributes to the system could be found. The geometric features considered in this study are the shear span and effective depth of the pier cap. Change in concrete strength and reinforcement ratio also considered in this study. In order to verify the result of finite element model, the pier caps were reanalyzed by a strut and tie model. ABAQUS general purpose finite element software has been used for parametric study. After several trials the mesh passed all the quality tests and the analysis is done, ABAQUS checks whether any badly shaped elements exist. There were no such warning messages in the analysis progress window or in the standard output file, so it"s possible to inspect and accept the analysis results. The results obtained were presented in the next sections.

4.3 EFFECT OF CHANGE IN CONCRETE STRENGTH

This part of analysis concentrates on how change in concrete strength affects the performance of pier caps. The output of this analysis was presented for each pier caps for varying concrete strength as follows.

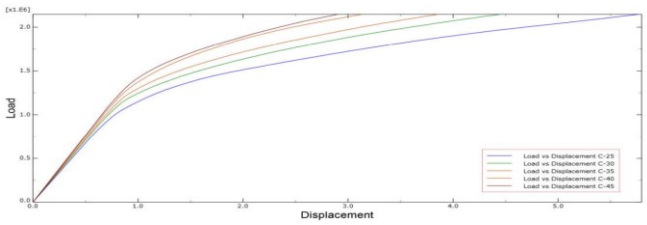

Figure 4.11 load vs. displacement graph for different concrete strength

As the concrete strength increases, the displacement decreased in pier caps of three dimensional models subjected to concentrated bearing load. It can be understood that improving the concrete grade increases the caring capacity of pier caps in terms of minimizing deflection.

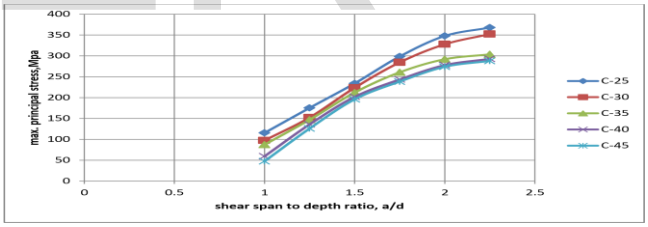

Figure 4.12 Maximum principal stresses with variable concrete strength

As shown from Figure 4.12, for identical shear span to effective depth ratio the stresses were maximum for a lesser concrete grade and it increases as the shear span to effective depth ratio increases, this means that a pier cap with minimum concrete grade and higher shear span to effective depth ratio experiences maximum stress and displacement. As concrete strength varies from C-25 to C-45, both the displacement resultant and the maximum principal

stress were decreased. There were 49.6% and 28.2% decrease in displacement resultant and the maximum principal stress respectively

Effect of Change in Concrete Strength Using Strut and Tie Model

For pier caps with different shear span to depth ratio the shear capacities are predicted as shown in figure below for different concrete grades.

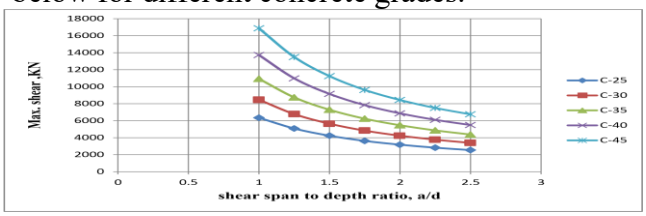

Figure 4.13 Effect of concrete cube strength on shear capacity of pier caps using STM method

It shows that as the shear span to effective depth ratio of a pier cap increases the shear capacity decreases. On the other hand shear capacity of pier caps increase as the concrete grade increases from C-25 to C-45.

4.4 EFFECT OF CHANGE IN GEOMETRY (a/d RATIO) ON THE BEHAVIOR OF PIER CAPS

This part of analysis concentrates on how change in geometry affects the performance of pier caps. The length and width of the pier caps are kept constant and the depth or the shear span to effective depth ratio was selected to be varied for the parametric study. The output of analysis for each pier caps with different shear span to depth ratios are presented as follows.

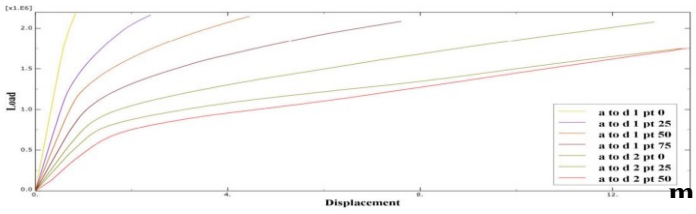

Figure 4.14 Load vs. displacement for different shear span to depth ratios

It can be understood from Figure 4.14 that as the shear span to effective depth ratio increases, the displacement resultant increased from 0.84mm to 12.87mm. Therefore from the concept of Figure 4.11, using higher concrete grades for pier caps with higher shear span to depth ratio can limit the maximum deflection and the maximum principal stresses that occur within the pier caps. Similarly using higher concrete grades for pier caps with smaller shear span to effective depth ratio increases the shear capacity of pier caps.

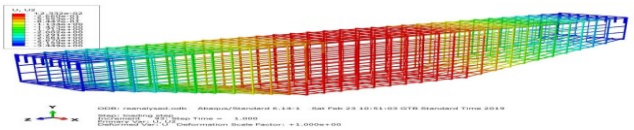

Figure 4.15 Reinforcement lay out in the pier cap

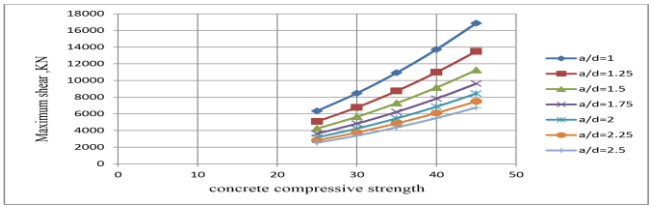

Figure 4.16 Effect of a/d ratio on shear capacity of pier caps using STM method It can be interpreted from the graph that as concrete strength increases the shear strength also increases where as the shear capacity of pier caps decrease as the shear span to effective depth ratio increases.

4.5 COMPARISON OF STM AND FEM

In this part of analysis, the study focuses on how the finite element method varies from the strut and tie model in the behavior of pier caps with respect to different shear span to effective depth ratio. For all the analyses conducted in this section of parametric study, the geometry of pier cap, material grade and loading condition are kept the same.

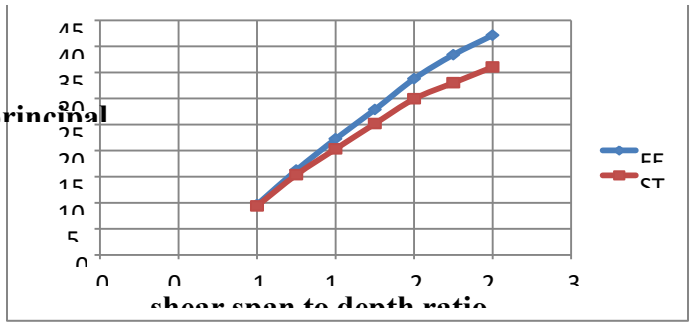

Figure 4.17 Maximum principal stresses with different analyzing method

The result of a finite element method of analyzing pier caps was compared with the strut and tie model. The maximum compressive principal stress with respect to a shear span to effective depth ratio for the finite element model and strut and tie model were presented graphically. The result shows that there was a maximum variation of

14.45% decrease in maximum compressive principal stress in STM as compared to FEM.

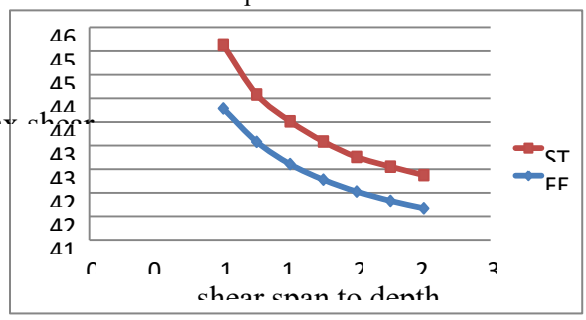

Figure 4.18 Maximum shears vs. shear span to depth ratio by varying method of analysis

From the graph, it can be seen that STM is successful in predicting the shear strength of pier caps. Hence this method can be successfully used to predict the shear strength behavior especially with respect to shear span to depth ratio (a/d) of pier caps.

4.6 EFFECT OF CHANGE IN REINFORCEMENT RATIO

In this part of analysis, the paper concentrates on how change in reinforcement ratio affects the performance of pier caps. For all the analyses conducted in this section of parametric study, the loading, material grades, modeling type, the depth and width of pier caps were kept the same. The results of this analysis were presented for each pier caps for varying reinforcement ratio as follows.

Table 4.7 Summary of analysis results with different reinforcement ratio.

Reinforcement ratio, ρ (%	Displacement resultant (mm)	Maximum principal stress,(Mpa)
0.40	6.652	336.8
0.45	6.189	287.3
0.60	4.243	240.4

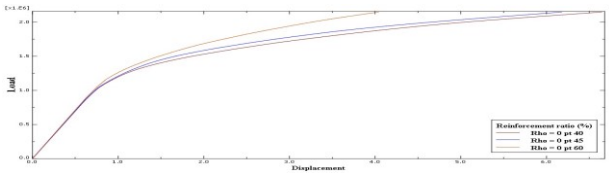

Figure 4.19 Load vs. displacement graph for different reinforcement ratios

From the results tabulated above, as the reinforcement ratio increases, both the displacement resultants and the maximum principal stress decreases. Similarly it can be understood from the graph that a pier cap with small reinforcement ratio experiences larger displacement.

5.CONCLUSION AND RECOMMENDATION

5.1 CONCLUSIONS

The conclusions drawn from this research are summarized as follows.

1. As the concrete strength increases, both the displacement and maximum principal stress decreased in pier caps of three dimensional models subjected to concentrated bearing loads. On the other hand the shear capacity of pier caps increase as the concrete strength increases. There were 49.6% and 28.2% decrease in displacement resultant and the maximum principal stress respectively.

2. The displacement resultant increased from 0.84mm to 12.87mm as the shear span to effective depth ratio increases from 1 to 2.5. However the shear capacity of the pier cap decreased with increase in shear span to effective depth ratio.
3. The compressive principal stress using a strut and tie model was lower than finite element method by 14.45%. But the prediction of

shear strength using finite element method is lower than that of strut and tie model.

4. As the longitudinal reinforcement ratio increase, both the displacement resultants and the maximum principal stress decreases by 36.2% and 28.62% respectively.
5. It was observed that the change in steel grade has no significant effect on the behavior of pier caps.
6. The flexural reinforcement area required using STM method is greater than that of sectional design approach by 14.3%.

5.2 RECOMMENDATION

1) Since there is no unique strut and tie model for a pier cap the designers can use any pattern of strut and tie members as per there interest and experience having in mind that the stress limits in the struts and nodal zones are satisfied. Therefore in order to get the optimal strut and tie model among different options, the designer can perform topology optimization technique by gradually removing inefficient material from a structure.
2) As a special concrete structure, there is no defined set of laws for designing pier caps in current Ethiopian codes except a little guidance in using strut and tie models provided on EBCS 2. The code lacks extensive coverage of STM design procedures as a result it is difficult to do a comprehensive parametric study. Providing clarification on STM in EBCS 2 will be very important. So that finite element method gives through insight for different parameters which affects the behavior of reinforced concrete pier caps.
3) The present study focuses on a numerical and analytical method of analyzing pier caps. Doing experimental investigation and comparing the result with finite element method can be taken up as an area of further work.

REFERENCES

AASHTO LRFD Bridge Design Specification. (2005). American Association of State Highway and Transportation Officials. Third Edition, Washington, D.C.

Andrew J. Bechtel (2011). External Strengthening of Reinforced Concrete Pier Caps. PhD thesis, Georgia Institute of Technology.

Barney T. Martin and David H. Sanders. (2007).Verification and Implementation of

Strut-and-Tie Model in LRFD Bridge Design Specifications. AASHTO, Highway Subcommittee on Bridge and Structures.

Ethiopian Road Authority (ERA). (2002). Bridge Design Manual, Addis Ababa, Ethiopia

Finotework Asnake. (2016). A Finite Element Method Based Analysis of Corbels. Master‟s thesis. Addis Ababa University.

Franz, G., and Niedenhoff, H. Reinforcement for Brackets and Short Beams.V.48, No.5, 1963, pp.112–120.

Gavin Macleod. (1997).Influence of concrete strength on the behavior of bridge pier caps. McGill University, Montreal.

Gerard P. and Nigel.H (2008). ICE manual of bridge engineering .institution of civil engineers, second edition.

H. Nilson et al. (2010). Design of concrete structures. Fourteenth edition. McGrawHill. America, New York.

Hemant Kumar Vinayak (2016) Direct Strut-And-Tie Model for Reinforced Concrete Bridge Pier Cap. Mathematical Modeling in Civil Engineering Vol. 12_ No. 1: 1_8.

Hong Yuan, Xingwei Xue and Shanqing Li. (2012).The Analysis and Experiment on

Key Technologies of Structural Design of Cap Beams of Highway Bridges. Mechanics and Materials.